

UNDERSTANDING THE FAILURE CHARACTERISTICS OF THE BEAM PERMIT SYSTEM OF RHIC AT BNL*

P. Chitnis[#], T.G. Robertazzi, Stony Brook University, NY, USA
 K. A. Brown, Brookhaven National Laboratory, NY, USA

Abstract

The RHIC Beam Permit System (BPS) monitors the anomalies occurring in the collider and restores the machine to a safe state upon fault detection. The reliability of the BPS thus directly impacts RHIC availability. An analytical multistate reliability model of the BPS has been developed to understand the failure development and propagation over store length variation. BPS has a modular structure. The individual modules have joint survival distributions defined by competing risks with exponential lifetimes. Modules differ in functionality and input response. The overall complex behavior of the system is analyzed by first principles for different failure/success states of the system. The model structure changes according to the type of scenario. The analytical model yields the marginal survival distribution for each scenario versus different store lengths. Analysis of structural importance and interdependencies of modules is also examined. A former Monte Carlo model [1] is used for the verification of the analytical model for a certain store length. This work is next step towards building knowledge base for eRHIC design by understanding finer failure characteristics of the BPS.

INTRODUCTION

The Beam Permit System (BPS) of Relativistic Heavy Ion Collider (RHIC) plays a key role in safeguarding against the developing faults in the collider. The energy stored in RHIC is about 2MJ in particle beams and 70 MJ in the form of magnet currents. Any abnormality in the machine can cause an undesirable escape of this energy, which can result into machine damage. BPS senses the onset of failures by monitoring the health inputs from RHIC support systems like power supplies, cryogenics, beam loss monitors, access controls, quench detection, vacuum system etc. In case of anomaly, it directs this energy out the machine for safe disposal.

RHIC reliability is directly dependent on the BPS reliability. Thus it is essential for the BPS to be highly reliable, being a safety critical system. Earlier a Monte Carlo (MC) model [1] was developed to quantify the probability of system level catastrophic events. This model simulated the behavior of modules with exponential competing failures. The module level failures were calculated by a quantitative fault tree analysis [2].

The MC model simulated the failure characteristics of the BPS for a certain store length. Also as the simulation

takes about 17 hours to run 1E9 iterations to generate reproducible results. It generated probabilities of system level failures for a particular store length. This paper is aimed towards developing a model that generates the system failure probabilities as a function of store length. We develop an analytical model of the BPS behavior using stochastic mathematics for this purpose.

RHIC BEAM PERMIT SYSTEM

The BPS has a modular structure that consists of 33 Permit Modules (PM) and 4 Abort Kicker Modules (AKM). These modules are connected by three fiber-optic links that run 10MHz carrier links whose presence signifies that the system is healthy. These links are called the Permit Link (PL), Blue Link (BL) and Yellow Link (YL). The PMs collect support systems' health inputs from the field, called Permit Inputs (PI) and Quench Inputs (QI). The PM takes decision to drop the carrier, indicating a failure. When there is a magnet system failure, QI goes bad, and all the three links are dropped. In case of any other failure PI goes bad and only the permit link is dropped. The carrier drop propagates to all the modules, resulting respectively in magnet power +beam dump and a beam dump only. The AKMs send the beam dump signal to the beam abort system. They have redundancy incorporated. For more details of BPS refer to [3]. Figure 1 shows the BPS configuration.

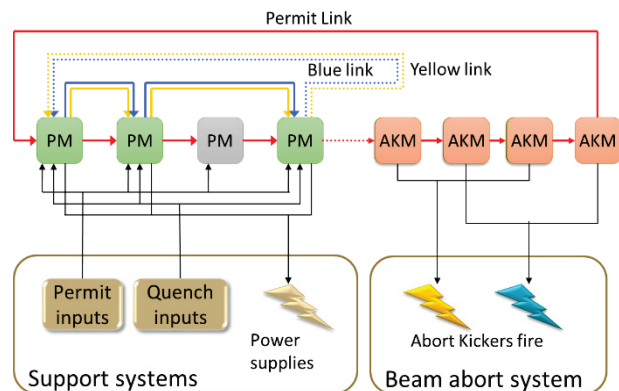


Figure 1: BPS connection diagram

SURVIVAL DISTRIBUTION

The PMs and AKMs have been analysed for their failure modes in [2]. The top level failure of BPS depends upon the states of the PMs and AKMs. The calculation

*Work supported by Brookhaven Science Associates, LLC under Contract No. DE-SC0012704 with the U.S. Department of Energy.
[#]prachi.chitnis@stonybrook.edu

showed that the top level failures of the modules have exponential survival distribution, which is characterized by a constant hazard function λ . Modules can have these failure states, False Beam Abort (F), a False Quench (M), Blind (B) and Dirty Dump (D), with failure rates as λ_F , λ_M , λ_B and λ_D resp. The PMs have {F, M, B} or {F, B} failure modes (green PM and grey PM resp. in Fig. 1). The AKMs have {F, M, D}. The inputs PI and QI are modelled as Poisson variable with exponential trigger rate as λ_{PI} and λ_{QI} . The initial state is a Good (G) state, where the module performs its intended function properly. The Markov diagrams for states is shown in Fig. 2.

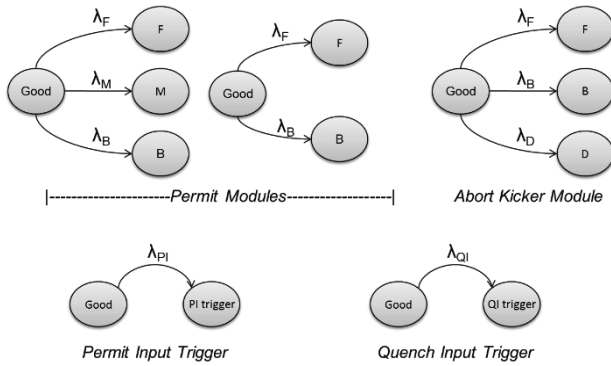


Figure 2: Markov diagrams

A competing risks model with crude lifetimes [1] [4] is implemented here, where multiple risks compete with each other to cause a final failure. Mathematically if a module is subjected to $j = \{1, 2, \dots, k\}$ risks, where $j = \{F, M, B\}$ for PMs, and $j = \{F, B, D\}$ for AKMs. The crude probability distribution function of risk j is given by

$$F_j(t) = \frac{\lambda_j}{\sum_{i=1}^k \lambda_i} (1 - e^{-(\sum_{i=1}^k \lambda_i)t}); j = \{1, 2, \dots, k\}$$

The marginal hazard rate for j^{th} risk is λ_j and t is the time of observation or the beam store length. The survival function for the module undergoing competing risks is given by

$$S_T(t) = e^{-(\sum_{i=1}^k \lambda_i)t}$$

At any given instant for a module, following expression is always true

$$S_T(t) + \sum_{j=1}^k F_j(t) = 1 \tag{1}$$

ANALYTICAL MODEL

The BPS has a ring configuration. A trigger arrival at a module initiates a carrier failure, which returns back to it after traversing all the modules in the system. The functionality of BPS that affects the reliability is to abort the beams and dump the magnet power upon trigger arrival. We thus cut out this ring configuration to a linear structure, with inputs and outputs. The start of this structure is the master module [3] and the end is the AKMs that abort the beam. We approach the problem of

developing mathematical equations for system states by looking at the states of each module in this system (Fig. 2). These states are of two kind: trigger state that initiates carrier failure (F, M) and passive state where a module waits in that state for a trigger (B, D, G). PI and QI are also the triggers to the system that initiate a carrier failure. For this reason we always use the failure density function $p(t)$ (instantaneous probability) for triggering state and failure distribution function $P(t)$ (probability that an event has occurred till now) for passive states to derive the expressions for the system level failures. For m^{th} module, and j^{th} triggering state where $j = \{F, M, PI, QI\}$

$$p_j^m(t) = \lambda_j e^{-(\sum_{i=1}^k \lambda_i)t}; P_j^m(t) = \int_0^t p_j^m(t) dt$$

For j^{th} passive failure state where $j = \{B, D\}$

$$P_j^m(t) = \frac{\lambda_j}{\sum_{i=1}^k \lambda_i} (1 - e^{-(\sum_{i=1}^k \lambda_i)t});$$

For passive good state

$$P_G^m(t) = e^{-(\sum_{i=1}^k \lambda_i)t}$$

Similar to Eq. 1, for a module m , at any given instant

$$P_G(t) + \sum_j (P_j^m(t)) = 1$$

Using above equations for modules' states, we further develop the analytical equations for the system states. BPS modules are connected by multiple links and some of the modules do not have blue/yellow link connected to them. We thus simplify the structure of BPS (shown in Fig. 1) for different type of system states. Also because AKM exhibit redundancy, we treat them as a separate entity that receive the signals from rest of the BPS. Consider the following configurations named I, II and III shown in Fig 3. Config. I shows the path of permit link triggers i.e. F and PI. Config. II shows the path of quench link triggers i.e. M and QI. Config. III shows the redundant configuration of the AKMs that signals the beam abort system to dump the beams.

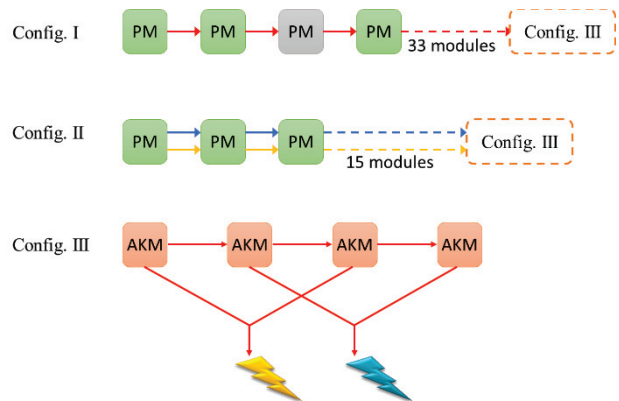


Figure 3: BPS connection diagram

Pre-Press Release 23-Oct-2015 11:00

Copyright © 2015 CC-BY-3.0 and by the respective authors

To develop equations for system states, we consider the probability of each module and one by one traverse the path of carrier failure to beam abort system output. Because of the complexity and length of the expressions, we avoid writing them in this paper. However we explain the strategy that we chose to develop them. Following are the system states that can result from combinations of module states.

- ND: No Dump - No trigger generated in I, II and III
- GD: Good Dump - Trigger PI arrives in I, or QI arrives in II. No other triggers are generated anywhere else. Signal goes to the output of III, all modules in the forward path are in G state.
- FD: False Beam Abort Dump - Trigger F arrives in I or III. No other triggers are generated anywhere else. Signal goes to the output of III, all modules in the forward path are in G state.
- MD: False Magnet Quench Dump - Trigger M arrives in II. No other triggers are generated anywhere else. Signal goes to the output of III, all modules in the forward path are in G state.
- BD: Blind Dump - Trigger F/PI arrives in I, or M/QI arrives in II, or trigger F arrives in II. Signal does not to the outputs of III, at least one module in the forward path is in B state.
- DGD: Dirty Good Dump - Trigger PI arrives in I, or QI arrives in II. No other triggers are generated anywhere else. Signal goes the output of III, with at least one output passing through the D state of redundant AKMs.
- DFD: Dirty False Beam Abort Dump - Trigger F arrives in I or III. No other triggers are generated anywhere else. Signal goes the output of III, with at least one output passing through the D state of redundant AKMs.
- DMD: Dirty False Magnet Quench Dump - Trigger M arrives in II. No other triggers are generated anywhere else. Signal goes the output of III, with at least one output passing through the D state of redundant AKMs.

RESULTS

The expressions are solved in Mathematica [5] and the time dependent probabilities functions for each scenario are calculated. These probabilities are verified with the help of Monte Carlo simulation reported in [1]. The failure rates of the modules are obtained from [2]. Some of the module failure rates are very small, especially B and D, which reflect at system level failures. Also due to the AKM redundancy, the DGD, DFD and DMD failure probabilities are much smaller. The Monte Carlo simulation will need a large number of iterations to verify these results. Thus we first assign hypothetical failure rates to all the modules, with specific high failure rates for D mode to overcome the redundancy effect, and get substantial number of DGD, DFD and DMD states for the verification. Also we assume a hypothetical store length $t = 0.232$ hours. The Monte Carlo simulation is run for

2.4E9 iterations and takes about 40 hrs to generate results. The probability is expressed as the number of system scenario generated / total no of system runs. Table 1 compares these hypothetical results from the Monte Carlo and the analytical model (7 digit precision)

Table 1: Verification of the analytical model by Monte Carlo results

Abbr.	Analytical	Monte Carlo
$P_{ND}(t)$	0.0149852	0.0149856
$P_{GD}(t)$	0.0621532	0.0621708
$P_{FD}(t)$	0.3105783	0.3105881
$P_{MD}(t)$	0.2494602	0.2494724
$P_{BD}(t)$	0.2754812	0.2754846
$P_{DGD}(t)$	0.0087564	0.0087507
$P_{DFD}(t)$	0.0406134	0.0406134
$P_{DMD}(t)$	0.0379719	0.0379183
Total (from model)	1.0000000	1.0000000

The individual probabilities of each scenario from the analytical model is very close to the probabilities obtained from the Monte Carlo. The exact sum of all the probabilities from the models is 1 as shown in the table. This verifies that the relative probability expressions for a model considers all possible states in which the BPS can go.

This establishes that the analytical model and the Monte Carlo model both are verified. Next we put the actual failure rates in the analytical model and obtain the actual failure probabilities of the all the system states, with the store length equal to 6 hrs as RHIC average store length.

$$\begin{aligned}
 P_{ND}(t) &= 0.143573 \\
 P_{GD}(t) &= 0.856193 \\
 P_{FD}(t) &= 0.000123713 \\
 P_{MD}(t) &= 0.000101377 \\
 P_{BD}(t) &= 7.74551 E - 6 \\
 P_{DGD}(t) &= 1.39145 E - 6 \\
 P_{DFD}(t) &= 1.99945 E - 10 \\
 P_{DMD}(t) &= 1.64755 E - 10
 \end{aligned}$$

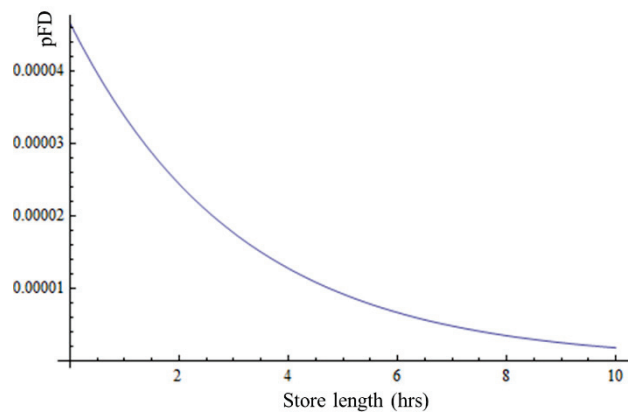


Figure 4: Probability density for FD system failure

Fig. 4, Fig. 5 and Fig. 6 show the graphs for the probability densities of three important system level failures (FD, MD and BD) plotted as a function of store length. The probability values above are cumulative values and can be calculated as the area under the curve up to a certain store length.

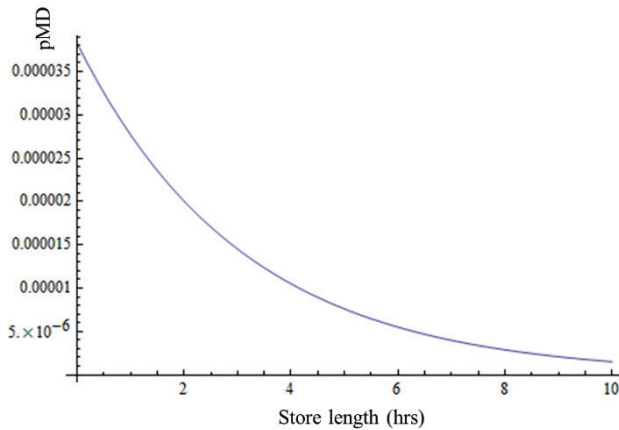


Figure 5: Probability density for MD system failure

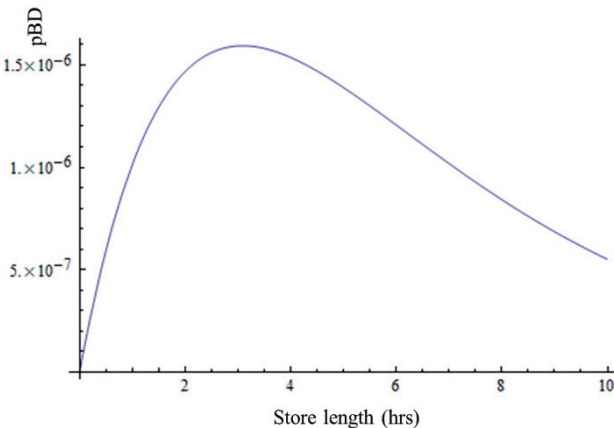


Figure 6: Probability density for BD system failure

DISCUSSION

There are certain advantages of deducing the mathematical expressions for the probabilities of system level states. It facilitates quicker and easier analysis of the variation in system failure probabilities with change in component failure distributions or PI/QI trigger rates.

We utilize this to analyze the importance and interdependency of individual modules. The importance of the modules is evaluated as a combined effect of their failure rate magnitude and structural position. We analyze the three major system failure states, FD, MD and BD. The procedure is to increase the failure rates of F, M and B modes for each module one by one, and observing the change in the system failure probabilities, which is an

indicator of the importance of the module. To summarize this comprehensive analysis, we can say that a module's importance is highly dependent on its failure rate. Alongside structural placement also plays a key role in determining the importance. The modules which are in the path of propagation of multiple failures have higher importance. The nearer a module is to the abort system output, higher is its importance. This is because probability of it being bypassed in failure propagation is small. The AKMs have lower importance due to the redundancy incorporated. Components that are major contributors to higher failure rate are discussed in [2].

To assess the interdependency between the modules, the modules are ordered according to their importance. After this we increase the failure rate for the subsequent module pairs, and observe the increase the system level failure probabilities. For no dependency, the system failure should have the same order for importance of modules for pairs [6]. We do not find any interdependency in the modules.

CONCLUSION

We develop a mathematical model for understanding the fine failure characteristics of the BPS. After the verification of this mathematical model through a MC model developed earlier, we are able to probe deeply into the failure probability distributions. This provides us with a faster way to analyze the system failures with change in system configuration. This model will provide a vision for the design of protection systems for the upcoming eRHIC project at BNL [7].

REFERENCES

- [1] P. Chitnis et al., "A Monte Carlo simulation approach to the reliability modeling of the beam permit system of RHIC at BNL", ICALEPCS 2013, San Francisco
- [2] P. Chitnis et al., "Quantitative fault tree analysis of the beam permit system elements of RHIC at BNL", ICALEPCS 2013, San Francisco
- [3] C.R. Conkling, "RHIC Beam Permit and Quench Detection Communication System", Proceedings of the Particle Accelerator Conference, 1997
- [4] M.J. Crowder, *Classical Competing Risks*, 2001, Chapman & Hall/CRC
- [5] Wolfram Research Inc., *Mathematica*, Version 9, Champaign, IL (2014).
- [6] S.T. Rachev, Professor of Finance, Stony Brook University, *Private Communication*, 2014
- [7] V. Ptitsyn et al., "eRHIC, A Future Electron-Ion Collider at BNL", Proceedings of the 9th EPAC, Lucerne, 2004